Cancer Cell
Article

Naturally Occurring Neomorphic *PIK3R1* Mutations Activate the MAPK Pathway, Dictating Therapeutic Response to MAPK Pathway Inhibitors

Lydia W.T. Cheung,[1,*] Shuangxing Yu,[1] Dong Zhang,[1] Jie Li,[1] Patrick K.S. Ng,[1] Nattapon Panupinthu,[1,4] Shreya Mitra,[1] Zhenlin Ju,[1,2] Qinghua Yu,[1] Han Liang,[2] David H. Hawke,[1,3] Yiling Lu,[1] Russell R. Broaddus,[3] and Gordon B. Mills[1]
[1]Department of Systems Biology
[2]Department of Bioinformatics and Computational Biology
[3]Department of Pathology
University of Texas MD Anderson Cancer Center, Houston, TX 77030, USA
[4]Department of Physiology, Faculty of Science, Mahidol University, Bangkok 10400, Thailand
*Correspondence: wcheung@mdanderson.org
http://dx.doi.org/10.1016/j.ccell.2014.08.017

SUMMARY

PIK3R1 (p85α regulatory subunit of PI3K) is frequently mutated across cancer lineages. Herein, we demonstrate that the most common recurrent *PIK3R1* mutation *PIK3R1*^{R348*} and a nearby mutation *PIK3R1*^{L370fs}, in contrast to wild-type and mutations in other regions of *PIK3R1*, confers an unexpected sensitivity to MEK and JNK inhibitors in vitro and in vivo. Consistent with the response to inhibitors, *PIK3R1*^{R348*} and *PIK3R1*^{L370fs} unexpectedly increase JNK and ERK phosphorylation. Surprisingly, p85α R348* and L370fs localize to the nucleus where the mutants provide a scaffold for multiple JNK pathway components facilitating nuclear JNK pathway activation. Our findings uncover an unexpected neomorphic role for *PIK3R1*^{R348*} and neighboring truncation mutations in cellular signaling, providing a rationale for therapeutic targeting of these mutant tumors.

INTRODUCTION

Specific molecular aberrations in a cancer gene can have functional consequences that determine therapeutic sensitivity (Chen et al., 2004; Lutzky et al., 2008; Lynch et al., 2004). Importantly, specific mutations can exhibit hypomorphic (decreased function), hypermorphic (increased function), or less understood neomorphic (gain-of-function) effects. Indeed, mutated *IDH1* and *IDH2* and a number of other oncogenic mutations are neomorphs (Ward et al., 2010). If neomorphic mutations are common in human tumors, this will require a systematic characterization of underlying mechanisms and therapeutic liabilities engendered by the neomorphic mutations if we are to optimally capitalize on broad genomic characterization of patient tumors and implementation of personalized cancer therapy.

PIK3R1 mutation represents one of the most common aberrations being the 11th most commonly mutated gene across 4,429 tumors covering 20 diseases in The Cancer Genome Atlas (TCGA) database. *PIK3R1* mutations are particularly prevalent in endometrial (20% and 34% in our and TCGA data sets, respectively; Cheung et al., 2011; Kandoth et al., 2013) and colon cancers (4%; TCGA; Cerami et al., 2012). We recently demonstrated that the most common recurrent *PIK3R1* mutation, R348*, which accounts for approximately 10% of all *PIK3R1* mutations in endometrial and colon cancers, acts as a gain-of-function mutation by increasing survival in BaF3 murine myeloid cells (Cheung et al., 2011). *PIK3R1*, which encodes the p85α subunit of PI3K, functions primarily as a regulator of the p110α catalytic product of the *PIK3CA* locus. Importantly, the *PIK3R1*^{R348*} truncation mutation produces a protein that cannot bind to p110α and thus the gain-of-function activity of *PIK3R1*^{R348*} is unlikely to involve altered p110α activity. Whether additional patient-derived mutations in *PIK3R1* in proximity to R348 (Cerami et al., 2012; Cheung et al., 2011) will also act as gain-of-function mutations is not yet known. Based on the frequency of *PIK3R1*^{R348*} and neighboring mutations as well as

Significance

Previously characterized mutants of the p85α regulatory subunit of PI3K exclusively target PI3K pathway activation either by activating p110 or decreasing PTEN function. We demonstrate that *PIK3R1*^{R348*} and neighboring truncation mutations are neomorphs that result in selective activation of components of the MAPK pathway leading to therapeutic sensitivity to MEK and JNK inhibitors. These neomorphic mutations represent the most common subset of recurrent *PIK3R1* mutations in endometrial and colon cancers and could potentially be biomarkers of responsiveness to inhibitors targeting the ERK and JNK pathways in tumors with these mutations. Our findings also suggest that the selection of targeted therapies may need to be conditioned on the specific mutation in the cancer gene rather than on the cancer gene alone.

the gain-of-function activity of *PIK3R1*^{R348*}, we investigated the functional consequences of *PIK3R1* mutations within the region on cellular signaling and cellular phenotypes as well as therapeutic liabilities.

RESULTS

PIK3R1^{R348*} and *PIK3R1*^{L370fs} Render Cells Sensitive to Specific MAPK Pathway Inhibitors

Having previously demonstrated that *PIK3R1*^{R348*} is a gain-of-function mutation in BaF3 cells, we undertook a BaF3 differential cytotoxicity screen to examine whether specific *PIK3R1* mutations would alter sensitivity toward a collection of 145 compounds targeting major signaling pathways. The normally interleukin 3 (IL-3)-dependent BaF3 cells were rendered IL-3-independent by stable expression of p85α mutants that activate signaling pathway(s) able to drive survival of BaF3. Inhibitors that target signaling pathway(s) induced by the mutant would cause growth inhibition or cell death that can be rescued by exogenous IL-3, providing a "counterscreen" for nonspecific effects of the inhibitor. The inhibiting concentration 25% (IC_{25}) and inhibiting concentration 50% (IC_{50}) values for each compound across the cell lines are listed in Table S1 (available online). Strikingly, *PIK3R1*^{E160*} and *PIK3R1*^{R348*} mutations rendered the cells sensitive to different PI3K pathway inhibitors (Figure S1A). Exogenous IL-3 rescued cells from the inhibition, consistent with an on-target effect as compared to nonspecific toxicity. Interestingly, *PIK3R1*^{E160*}, which we have demonstrated to alter PTEN stability and activity (Cheung et al., 2011), led to sensitivity to a downstream inhibitor of the pathway (rapamycin) but not an inhibitor of p110 (GDC0941), which is proximal to PTEN. In contrast, *PIK3R1*^{R348*} engendered sensitivity to an AKT inhibitor MK2206, but not rapamcyin or GDC0941. If this sensitivity is reflected in patient tumors, differential therapeutic approaches will be required for these and potentially other *PIK3R1* mutations. Intriguingly, *KRAS*^{G12D}-expressing BaF3 cells were sensitive to rapamycin and MK2206 potentially due to the interaction of KRas G12D with p110 (Rodriguez-Viciana et al., 1994).

The advantage of probing the cell lines with a large "informer" library is the potential to identify unexpected therapeutic liabilities. Indeed, BaF3 cells expressing *PIK3R1*^{R348*} were sensitive to multiple MEK (PD0325901, AZD6244, PD98059, CI1040, and hypothemycin) and JNK inhibitors (SP600125, BI78D3, and AEG3482; Figure 1A; Figure S1A), which was again reversed by IL-3. Strikingly, sensitivity to MEK and JNK inhibitors was not altered in cells expressing *PIK3R1*^{E160*} or known gain-of-function *PIK3R1* mutations (DKRMNS560 del, R574fs, and T576 del; Cheung et al., 2011; Quayle et al., 2012; Figure 1A; Figures S1A and S1B). In contrast, *KRAS*^{G12D} conferred sensitivity to MEK and p38 MAPK inhibitors, but not JNK inhibitors (Figure 1A; Figure S1A). Furthermore, the oncogenic *PIK3CA*^{E545K} and *PIK3CA*^{H1047R} mutants did not alter sensitivity to the MAPK pathway inhibitors (Figure S1B).

To investigate whether truncation mutations neighboring R348 also confer sensitivity to MAPK pathway inhibitors, we used an ovarian endometrioid cancer cell line OVK18, which carries a naturally occurring *PIK3R1*^{L370fs} mutation (see Figure 4D below for mapping of the region required to mediate the effects engendered by *PIK3R1*^{R348*}). Consistent with the BaF3 screen, OVK18 was sensitive to multiple MEK and JNK inhibitors, but not to the p38 MAPK inhibitor (Table 1). Ovarian endometrioid cancer is similar to endometrial endometrioid cancer and indeed is thought to arise from endometriosis in the ovary (Ness, 2003), we therefore compared OVK18 with a series of endometrial endometrioid cancer cell lines. Intriguingly, endometrial endometrioid cancer cell lines without *PIK3R1*^{L370fs} but with mutations in PI3K and MAPK pathways that parallel those in OVK18 were less sensitive to MAPK pathway inhibitors (Table 1; Table S3). These results are consistent with the endogenous *PIK3R1*^{L370fs} mutation mimicking *PIK3R1*^{R348*} by rendering cells sensitive to MAPK pathway inhibitors.

PIK3R1^{R348*} and *PIK3R1*^{L370fs} Induce ERK and JNK Activation

We next determined whether pathway activation correlates with drug sensitivity. Consistent with the sensitivity to MEK inhibitors, reverse-phase protein arrays (RPPA) revealed elevated levels of phosphorylated MKK1 (upstream kinase of ERK1/2) in BaF3 cells expressing *PIK3R1*^{R348*} or *KRAS*^{G12D} (Figure 1B; Figure S1C; Table S2). In contrast, elevated phosphorylated JNK1/2 (p-JNK) and phosphorylated c-Jun (p-c-Jun; downstream substrate of JNK) occurred exclusively in *PIK3R1*^{R348*}-expressing BaF3, whereas phosphorylated p38 MAPK (p-p38 MAPK) was modestly increased in *KRAS*^{G12D} cells. Western blots confirmed that *PIK3R1*^{R348*} and *KRAS*^{G12D} markedly increased phosphorylation of MKK1, ERK1/2 and the downstream substrate p90RSK (Figure 1C). *PIK3R1*^{R348*} increased phosphorylation of JNK and c-Jun but not p38 MAPK, which was, as predicted, phosphorylated in cells expressing *KRAS*^{G12D}. In contrast, *PIK3R1* mutants (including *PIK3R1*^{E160*}) and *PIK3CA* mutants that had no effect on sensitivity to MAPK inhibitors did not alter phosphorylation of MAPK pathway members (Figure 1C; Figures S1D and S1E).

Strikingly, ERK and JNK were activated upon serum starvation or growth factor stimulation in *PIK3R1*^{L370fs} mutant OVK18 cells (Figure 2A). Note the expression of the truncation mutation in OVK18 cells). As expected, p-p38 MAPK remained unaltered. Importantly, the activation of ERK and JNK were mediated by *PIK3R1*^{L370fs} because two p85α siRNAs that efficiently knocked down the L370fs protein decreased ERK and JNK phosphorylation (Figure 2A). In contrast, a siRNA that decreased expression of WT p85α but not the L370fs mutant failed to decrease ERK and JNK activation. It is noteworthy that although *PIK3R1*^{L370fs} induced MAPKs activation, the mutant protein was present at low levels compared to WT p85α in OVK18, consistent with *PIK3R1*^{L370fs} acting as a gain-of-function mutation.

To further assess the generalizability of effects of *PIK3R1* mutants on MAPK pathway activation, we expressed the mutants in a series of endometrial cancer cell lines with WT RAS genes. *PIK3R1*^{R348*} increased phosphorylated ERK (p-ERK) and p-JNK levels in all four endometrial cancer cell lines assessed (Figure 2B; Figure S2A; Table S3). *KRAS*^{G12D}-transfected cells showed increase in p-ERK and p-p38 MAPK. Once again, *PIK3R1* mutants that did not alter sensitivity to MAPK inhibitors did not increase phosphorylation of MAPKs (Figure 2B; Figure S2A), reinforcing the notion that activation of pathway underlies drug sensitivity and highlighting the neomorphic function of *PIK3R1*^{R348*} and *PIK3R1*^{L370fs}. Activation of the MAPK pathway

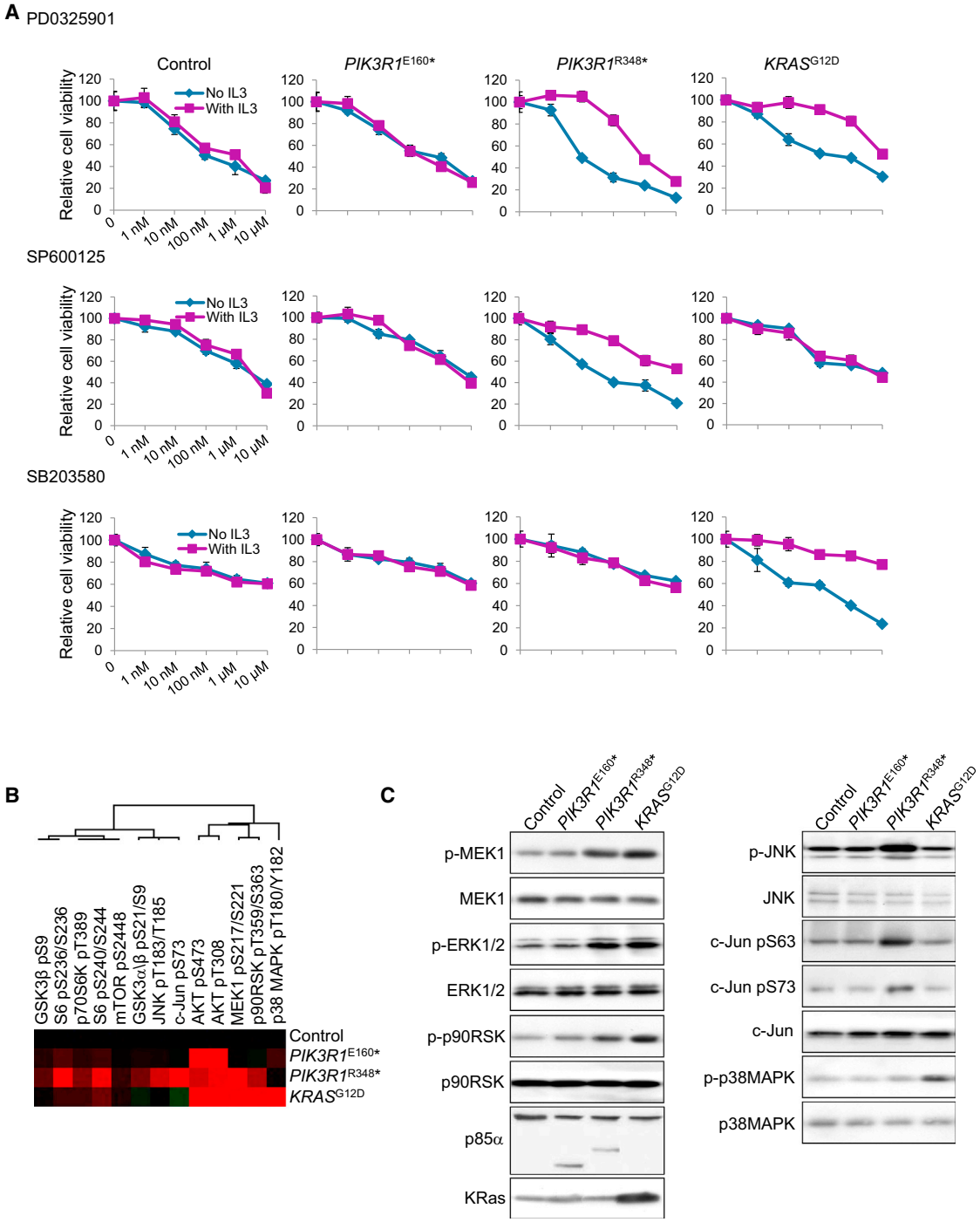

Figure 1. *PIK3R1*^{R348} -Expressing Cells Display Preferential Sensitivity to MAPK Inhibitors and Elevated ERK and JNK Phosphorylation

(A) Dose-response curve of control BaF3 cells (Control), which was established after transfection of *PIK3R1*^{WT} but expressed low exogenous WT p85α level, or BaF3 cells stably expressing *PIK3R1*^{E160*}, *PIK3R1*^{R348*}, or *KRAS*^{G12D} for PD0325901, SP600125, and SB203580. Means (±SD) of duplicates from two independent experiments are shown.

(B) Heatmap of unsupervised cluster analysis of stable BaF3 cells and selected proteins by RPPA. Red indicates higher level relative to other samples.

(C) The same set of lysates used in (B) was used for western blotting.

See also Figure S1 and Tables S1 and S2.

by *PIK3R1*^{R348*} and *PIK3R1*^{L370fs} is independent of the canonical role of p85α in PI3K signaling because multiple PI3K pathway inhibitors (GDC0941, PI103, and MK2206) that effectively inhibited *PIK3R1*^{R348*}- and *PIK3R1*^{L370fs}-induced AKT phosphorylation did not decrease phosphorylation of ERK and JNK (Figures S2B and S2C).

Table 1. IC_{25} and IC_{50} Values for MAPK Inhibitors in Tested Cell Lines

		MEK Inhibitor (IC_{25}/IC_{50})					JNK Inhibitor (IC_{25}/IC_{50})			p38 MAPK Inhibitor (IC_{25}/IC_{50})
	tumor type	AZD6244	PD98059	PD0325901	U0126	GSK1120212B	SP600125	BI78D3	AS601245	SB203580
ECC1	endometrial	3.1/NA	5.5/NA	7.1/NA	0.2/NA	1.4/NA	NA/NA	NA/NA	NA/NA	NA/NA
HEC108	endometrial	9.8/NA	NA/NA	5.5/NA	0.6/NA	0.6/NA	NA/NA	4.1/NA	2.3/NA	NA/NA
HEC265	endometrial	NA/NA	NA/NA	NA/NA	1.4/NA	NA/NA	NA/NA	NA/NA	1.1/NA	NA/NA
SNGII	endometrial	0.1/NA	0.4/NA	2.1/NA	0.6/7.8	1.3/NA	NA/NA	1.1/NA	0.49/9.8	NA/NA
OVK18	ovarian	0.03/1.2	0.03/2.7	0.04/1.8	0.009/0.7	0.04/9.5	0.09/7.1	0.06/8.2	0.08/6.4	NA/NA

IC_{25} and IC_{50} values presented in micromoles; NA, not available, inhibition did not reach 25% or 50%.
See also Table S3.

PIK3R1^{R348*}-Bearing Endometrial Cell Lines and Tumors Have High Nuclear p-ERK and p-JNK

MAPKs traffic between cellular compartments to propagate signals. Subcellular fractionation showed that p-ERK was elevated in both the cytosol and nucleus in *PIK3R1*^{R348*}- and *KRAS*^{G12D}-expressing endometrial cancer cells (Figure 2B). In contrast, p-JNK was increased primarily in the nucleus of *PIK3R1*^{R348*}-expressing cells. Accumulation of nuclear p-c-Jun was also observed (Figure S2D), consistent with *PIK3R1*^{R348*} increasing nuclear JNK activity.

We were able to probe the effect of *PIK3R1*^{R348*} on p-ERK and p-JNK localization by immunohistochemistry of four *PIK3R1*^{R348*} mutant endometrial tumors which displayed strong nuclear staining of both p-ERK and p-JNK. In contrast, nuclear p-ERK and p-JNK staining of 12 non-*PIK3R1*^{R348*} endometrial tumors were less intense, regardless of mutations in other sites in *PIK3R1* and other genes in the PI3K pathway (Figures 2C and 2D; Table S4).

PIK3R1^{R348*} Activates Specific MAPK Kinases

MAPK kinases (MKKs) selectively activate different MAPKs (Dérijard et al., 1995). For instance, MKK7 exclusively activates JNK, whereas MKK4 activates p38 MAPK and JNK (Tournier et al., 1997). Consistent with the selective effects of *PIK3R1*^{R348*} and *KRAS*^{G12D} on phosphorylation of MAPKs, both *PIK3R1*^{R348*} and *KRAS*^{G12D} increased phosphorylated MKK1/2 (p-MKK1/2), which phosphorylates ERK (Figure 3A). In addition, knockdown of MKK1 and MKK2 by two independent siRNAs reversed *PIK3R1*^{R348*}- and *KRAS*^{G12D}-induced ERK phosphorylation (Figure 3B; Figures S3A and S3B). In contrast, phosphorylated MKK7 (p-MKK7) was induced by *PIK3R1*^{R348*}, whereas *KRAS*^{G12D} activated MKK3 and MKK4. Strikingly, knockdown of MKK7, but not MKK4, significantly decreased JNK phosphorylation induced by *PIK3R1*^{R348*} (Figure 3B; Figures S3A and S3B).

We further determined the localization of the activated MKKs. In *PIK3R1*^{R348*}-expressing cells, p-MKK1/2 located exclusively in the cytosol, whereas increased p-MKK7 could only be observed in the nucleus (Figure 3C). Intriguingly, *PIK3R1*^{R348*} also induced translocation of total MKK7 from the cytosol to the nucleus (Figure 3C) without altering total cellular levels (Figure 3A). The accumulation and activation of nuclear MKK7 is compatible with JNK being directly phosphorylated in the nucleus.

MKK1/2 is regulated by RAF family kinases. Knockdown of B-Raf decreased p-MKK1/2 and p-ERK induced by *PIK3R1*^{R348*} or *KRAS*^{G12D} (Figure 3D; Figures S3C and S3D). In contrast, c-Raf or A-Raf siRNAs had no detectable effect on *PIK3R1*^{R348*}-induced MKK1/2 or ERK phosphorylation although the proteins were efficiently depleted by the siRNAs and c-Raf siRNAs did decrease *KRAS*^{G12D}-induced p-MKK1/2 and p-ERK (Figure 3D; Figures S3D and S3E). In addition, B-Raf activation as indicated by phosphorylation at threonine and serine residues was increased in *PIK3R1*^{R348*}-expressing cells (Figure 3E). Thus B-Raf appears to be a critical intermediary between *PIK3R1*^{R348*} and ERK signaling activation.

The MLK serine/threonine protein kinase family including MLK2, MLK3 and DLK represents the dominant kinases for MKK7 (Gallo and Johnson, 2002). Importantly, siRNAs against MLK3, but not MLK2 or DLK, abolished *PIK3R1*^{R348*}-induced p-JNK (Figure 3F; Figures S3F and S3G). It is noteworthy that nuclear p-MKK7 was also decreased; however, depletion of MLK3 did not inhibit nuclear translocation of total MKK7, suggesting that MKK7 nuclear translocation is independent of MLK3 and MKK7 phosphorylation. *PIK3R1*^{R348*} induced a redistribution of MLK3 from the cytosol to the nucleus (Figure 3G). In addition, serine and threonine phosphorylated MLK3 was increased by *PIK3R1*^{R348*} exclusively in the nucleus, but not in the cytosol (Figure 3H). These data suggest that activation of JNK signaling by *PIK3R1*^{R348*} is initiated in the nucleus and this activation involves nuclear translocation and subsequent phosphorylation of MLK3 and MKK7.

p85α R348* and L370fs Localize to the Nucleus

Next, we investigated whether the localization of p85α R348* correlates with nuclear accumulation of MKK7 and MLK3. WT p85α and p85α E160* localized predominantly in the cytosol (Figures 4A and 4B). Strikingly, p85α R348* was readily detected in the nucleus. p85α L370fs, which activated ERK and JNK in OVK18, also localized to the nucleus (Figure S4A). Localization of p110α was not altered by WT p85α, which does not enter the nucleus or by p85α R348*, which does not bind p110 (Figure S4B).

To gain insight into mechanisms underlying nuclear translocation of p85α R348*, we mapped the domain that enables nuclear translocation using a series of truncation p85α mutants. Four truncation mutants downstream of R348* failed to translocate to the nucleus (Figures S4C–S4E). Furthermore, these four mutations failed to activate MAPKs or promote IL-3 independent survival of BaF3 (Figures S4F and S4G). Two mutants upstream of R348* between the BCR homology (BH) domain and the nSH2

domain, N299* and N324*, localized to the nucleus (Figures 4C and 4D; Figure S4H). Importantly, similar to *PIK3R1*^{R348*}, these two mutations induced p-ERK and p-JNK (Figure 4E) and IL-3-independent survival of BaF3 (Figure 4F). In contrast, truncation mutants within the BH domain (R188*, E212*, Q235*, E266*) did not translocate to the nucleus, induce MAPK phosphorylation, or mediate survival of BaF3.

To determine whether nuclear localization of p85α mutants was essential for activation of the JNK signaling cascade, a nuclear export signal (NES) was engineered into the N-terminal end of p85α R348* and p85α N324* to exclude them from the nucleus. These NES-containing mutants retained the ability to activate B-Raf, MKK1/2 and ERK (Figure 4G; Figures S4I and S4J), consistent with this occurring in the cytosol. In contrast, activation of the JNK signaling cascade, including phosphorylation of c-Jun, JNK, MKK7 and MLK3 was impaired in NES-containing mutants (Figures 4G and 4H). In addition, these NES-containing mutants did not induce nuclear translocation of MKK7 and MLK3 (Figure 4G). Taken together, these results reinforce the contention that p85α R348* mediates the nuclear accumulation of MLK3 and MKK7 thereby promoting activation of the JNK signaling cascade in the nucleus. In contrast, activation of ERK does not rely on nuclear localization of p85α R348*.

p85α R348* Translocates into the Nucleus through Binding to Cdc42 and Rac1, which Are Required for Activation of ERK and JNK

p85α does not contain a consensus intrinsic nuclear localization signal (NLS). As shown in Figure 4D, an intact BH domain appears to be necessary for nuclear localization of p85α mutants. This domain contains conserved motifs that bind small GTPases, including Cdc42 and Rac1 (Tolias et al., 1995; Zheng et al., 1994). Furthermore, Rac1 and Cdc42 contain canonical NLS and contribute to ERK and JNK activation (Etienne-Manneville and Hall, 2002; Teramoto et al., 1996), making these small GTPases plausible candidates to translocate R348* to the nucleus. As expected, an intact BH domain in WT and mutated p85α was required for binding to Cdc42 and Rac1 (Figure 5A). We did not detect RhoA binding to WT or mutant p85α. Remarkably, Cdc42 or Rac1 siRNAs, but not RhoA siRNAs, reduced nuclear p85α R348* levels (Figure 5B; Figures S5A–S5C) without affecting total p85α R348* levels (Figure S5D). Combined knockdown of Cdc42 and Rac1 further inhibited nuclear translocation of p85α R348* (Figure 5B; Figure S5C), suggesting that both Cdc42 and Rac1 contribute to nuclear translocation of p85α R348*.

Along with decreased nuclear translocation of p85α R348*, Cdc42, or Rac1 siRNAs inhibited nuclear translocation of MKK7 and MLK3 (Figure 5C; Figure S5E). These siRNAs also inhibited *PIK3R1*^{R348*}-induced phosphorylation of MLK3, MKK7, JNK, c-Jun, B-Raf, MKK1/2, and ERK, with combined knockdown producing a further reduction (Figures S5D, S5F, and S5G). Similar to siRNA, expression of dominant negative Cdc42 (T17N) or Rac1 (T17N) abrogated *PIK3R1*^{R348*}-induced ERK (Figures 5D and 5E) and JNK (Figures 5D and 5F) signaling cascades, suggesting a requirement for Rac1 and Cdc42 GTPase activities. Notably, nuclear translocation of p85α R348*, MKK7, and MLK3 was not abolished by dominant-negative Rac1 and Cdc42 (Figure 5D). Therefore, physical interaction with Cdc42 and Rac1 appears sufficient for nuclear translocation of p85α R348*, MKK7, and MLK3, whereas active Cdc42 and Rac1 are essential for initiation of the signaling cascade.

p85α R348* and L370fs Are Scaffolds for a MLK3/MKK7/JNK1/JNK2 Complex to Promote Nuclear JNK Signaling

Because Cdc42 and Rac1 are required for nuclear localization of p85α R348*, and R348*, in turn, is required for the nuclear translocation of MKK7 and MLK3, we speculated that these molecules exist as a complex in the nucleus. Indeed, p85α R348* co-immunoprecipitated with Cdc42, Rac1, MKK7, and MLK3 from nuclear extracts (Figures 6A and 6B). Interestingly, JNK1 and JNK2 were also present in the immunoprecipitates (Figures 6A and 6B). Notably, this nuclear complex formation was drastically reduced upon exclusion of p85α R348* from the nucleus by NES addition (Figure 6B), consistent with p85α R348* being required for assembly of a stable nuclear MLK3/MKK7/JNK1/JNK2 complex. The assembly of this nuclear complex was also observed in OVK18 in the context of p85α L370fs, but not in HEC108, where p85α did not localize to the nucleus (Figure S6A).

To further characterize the nuclear R348* complex, gel filtration experiments were conducted. Whereas a small portion of p85α R348* eluted in fractions 34–36, the majority of nuclear R348* was recovered in a large molecular complex (fractions 25–29), which also contained JNK1, JNK2, MKK7, MLK3, Cdc42, and Rac1 (Figure 6C). Immunoprecipitation confirmed that these proteins formed a physical complex in fractions 25–29, but not fractions 34–36 (Figure 6D). Strikingly, excluding R348* from the nucleus by NES addition led to an absence of detectable MKK7/MLK3 and JNK1/2 in fractions 25–26 and Cdc42/Rac1 in fraction 25 (Figure 6E). In the absence of nuclear p85α R348*, JNK1 coprecipitated with MLK3 and MKK7, but not JNK2, Cdc42, or Rac1 (Figure 6F). These results together support the notion that nuclear p85α R348* stabilizes a MLK3/MKK7/JNK1/JNK2 nuclear complex.

The p85α R348*/Cdc42/Rac1/MLK3/MKK7/JNK1/JNK2 Complex Can Be Detected in the Cytosol

To determine whether the JNK signaling complex could form in the cytosol and translocate to the nucleus, gel filtration and immunoprecipitation were also performed with cytosolic extracts. p85α R348* was present in fractions 29–33 and association of R348* with Cdc42, Rac1, and MLK3/MKK7/JNK1/JNK2 was detected in fraction 29, which was the only fraction where these molecules comigrated (Figures S6B and S6C). Excluding R348* from the nucleus resulted in cytosolic accumulation of R348*, MLK3, MKK7, JNK1, and JNK2 (fractions 25–29; Figure S6D). Interestingly the migration of Rac1 and Cdc42 was not altered, suggesting that these are normally part of large complex. Furthermore, all of the components of the complex were readily detectable by coimmunoprecipitation in fractions 25–29 (Figure S6E). Taken together, these results suggest that p85α R348* functions as a scaffold protein that assembles and stabilizes a complex of Cdc42, Rac1, MLK3, MKK7, and JNK1 and JNK2 in the cytosol. The stabilized complex then translocates to the nucleus for efficient and robust activation of the JNK pathway.

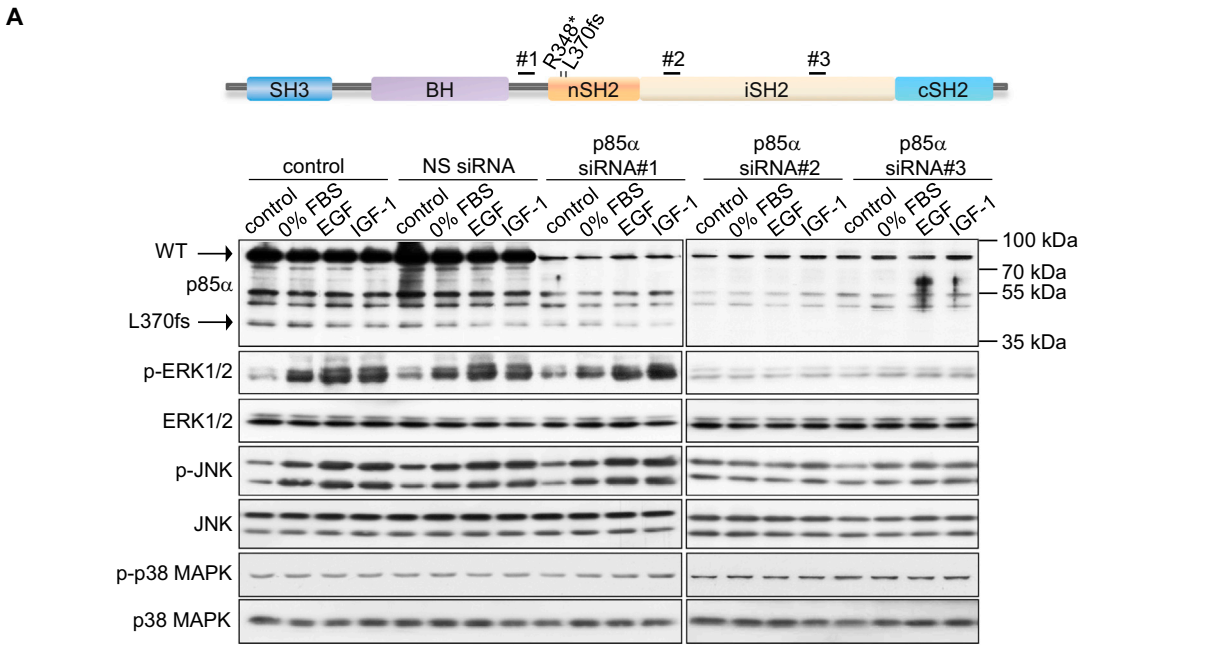

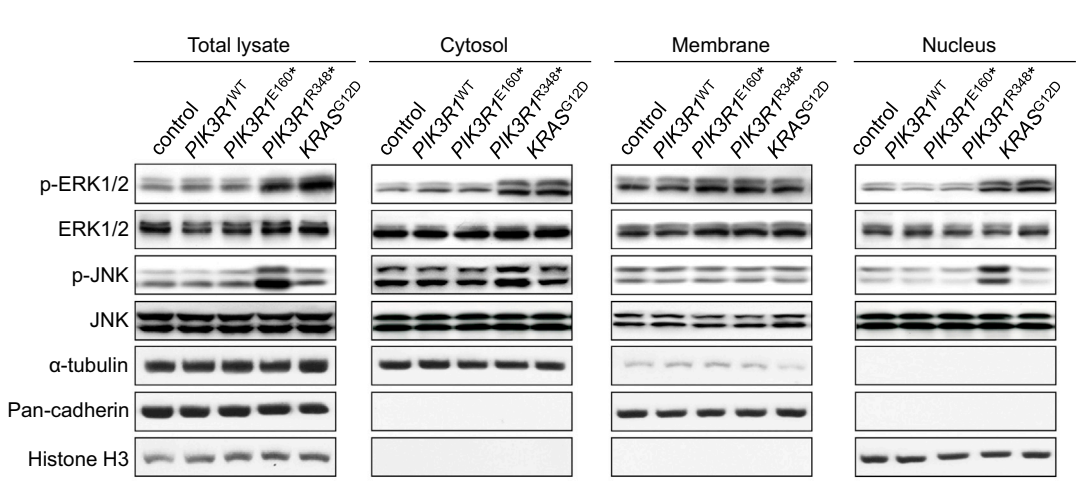

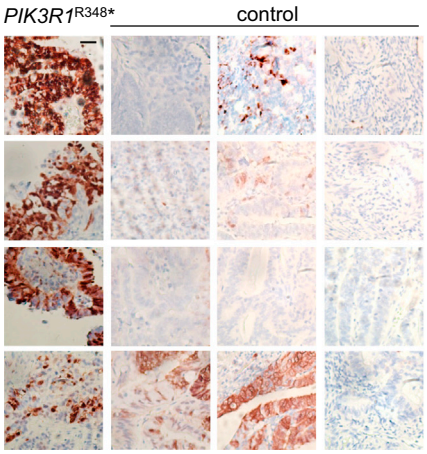

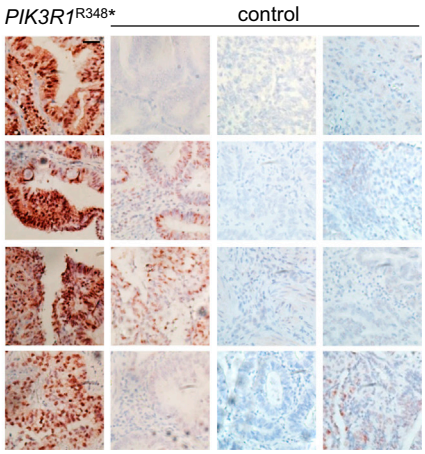

(legend on next page)

PIK3R1^{R348*} and *PIK3R1*^{L370fs} Promote Malignant Phenotypes through ERK and JNK Signaling In Vitro and In Vivo

To determine the functional relevance of ERK and JNK activation by *PIK3R1*^{R348*}, we established two independent stable endometrial cancer cell lines (Figure S7A) with results obtained from the two clones being essentially identical. *PIK3R1*^{R348*} stable clones demonstrated increased JNK and ERK phosphorylation (Figure S7A) as well as increased proliferation assayed by bromodeoxyuridine incorporation (Figure 7A), which was decreased by a MEK inhibitor, but not a JNK inhibitor (Figure 7A; Figure S7B), suggesting that *PIK3R1*^{R348*} induces proliferation through MEK/ERK activation. Inhibition of cell proliferation by the MEK or JNK inhibitor did not reach statistical significance in LacZ-, *PIK3R1*^{WT}-, or *PIK3R1*^{E160*}-expressing cells (Figure 7A; Figure S7B). The JNK pathway can induce or inhibit apoptosis depending on the cellular context. In the presence of FAS ligand, LacZ-, *PIK3R1*^{WT}-, or *PIK3R1*^{E160*}-expressing cells underwent apoptosis as indicated by DNA fragmentation (Figure 7B; Figure S7C). In contrast, *PIK3R1*^{R348*}-expressing cells were insensitive to this apoptotic stimulus. This anti-apoptotic effect was reversed by a JNK inhibitor, but not a MEK inhibitor (Figure 7B; Figure S7C), suggesting that *PIK3R1*^{R348*} protects cells from apoptosis through JNK activation. Strikingly, *PIK3R1*^{R348*} clones were 3-fold more invasive than *PIK3R1*^{WT} clones in Matrigel-coated Boyden chamber transwells (Figure 7C). Expression of *PIK3R1*^{R348*} also resulted in larger spheroids and higher cell viability in 3D Matrigel cultures (Figure 7D). These effects were suppressed by ERK and JNK inhibition (Figures 7C and 7D). Together, these data indicate that *PIK3R1*^{R348*} increases cells proliferation and invasion and decreases sensitivity to apoptosis through activation of ERK and JNK pathways.

To determine whether the in vitro effects on growth and invasiveness were recapitulated in vivo, LacZ-, *PIK3R1*^{WT}-, *PIK3R1*^{E160*}-, and *PIK3R1*^{R348*}-expressing isogenic endometrial cancer cell lines were injected subcutaneously into nude mice. Expression of *PIK3R1*^{R348*} significantly increased tumor growth as compared to LacZ- or *PIK3R1*^{WT}-expressing cells at week 3 ($p < 0.05$; Figure 7E). In accord with the in vitro and patient data, *PIK3R1*^{R348*}-expressing tumors showed marked elevation of p-ERK and p-JNK (Figure S7D). These *PIK3R1*^{R348*}-driven tumors were more sensitive to MEK and JNK inhibitors than *PIK3R1*^{WT}- and *PIK3R1*^{E160*}-expressing tumors as indicated by percent tumor growth inhibition (Figure 7F). Strikingly, OVK18 xenografts that have naturally occurring *PIK3R1*^{L370fs} were also highly sensitive to the MEK and JNK inhibitors (Figure S7E), further supporting the rationale for therapeutic targeting of *PIK3R1*^{R348*} or neighboring mutations with MAPK pathway inhibitors.

DISCUSSION

The effective implementation of targeted therapy ultimately lies in the individualization of treatment regimens based on effectively targeting the effects of driver mutations in cancer. Whereas current approaches focus on the discovery of targetable cancer genes, the drug screening and mechanistic studies herein suggest that the specific aberration in the cancer gene rather than the cancer gene alone should be considered for effective therapeutic targeting. The effect of particular mutations may not only demonstrate a quantitative effect on drug sensitivity but also a qualitative effect changing the function of the molecule and potentially requiring different therapeutic approaches (Chen et al., 2004; Lutzky et al., 2008; Lynch et al., 2004; Ward et al., 2010). We demonstrate that *PIK3R1*^{R348*} and the neighboring mutation *PIK3R1*^{L370fs} represent neomorphic p85α mutations that could potentially be biomarkers of responsiveness to inhibitors targeting the ERK and JNK pathways. Our observations that the naturally occurring *PIK3R1*^{L370fs} exhibited the same effects of *PIK3R1*^{R348*} strengthen the pathophysiological significance of the findings and more importantly indicate that *PIK3R1* truncation mutations in proximity to R348* exhibit the same phenotypes and therapeutic liabilities. Because *PIK3R1*^{R348*} is the most common recurrent *PIK3R1* mutations in endometrial cancers (9.6% and 6.9% of all *PIK3R1* mutations in our and TCGA data sets, respectively; Cheung et al., 2011; Kandoth et al., 2013) and colon cancers (16.6%; TCGA; Cerami et al., 2012) with multiple truncation and other mutations in *PIK3R1* in proximity, approaches to benefit patients with these aberrations are needed.

The primary function of p85 regulatory subunits is to stabilize and to maintain p110 catalytic subunits of PI3K in a quiescent state until activated by receptor tyrosine kinases (Cuevas et al., 2001; Yu et al., 1998). *PIK3R1*^{R348*} and *PIK3R1*^{L370fs} are different from the other naturally occurring *PIK3R1* mutations characterized because they activate not only the PI3K pathway, but also specific components of the MAPK pathway. The mechanism by which the PI3K pathway is activated warrants further investigation; this could be a result of interaction of the neomorphs with Cdc42 and Rac1, which can impinge on the PI3K pathway (Murga et al., 2002). However, the activation of the MAPK pathway by *PIK3R1*^{R348*} and *PIK3R1*^{L370fs} is independent of the conventional role of *PIK3R1* in PI3K signaling because the activation was insensitive to PI3K or AKT inhibitors. This is further

Figure 2. *PIK3R1*^{R348*}- and *PIK3R1*^{L370fs} Mutant Cell Lines and Endometrial Tumors Show High Levels of p-ERK and p-JNK

(A) Top, schematic showing the locations of p85α siRNA-targeted regions; Bottom, ovarian endometrioid cancer cells OVK18 transfected with p85α siRNAs or non-specific (NS) control for 72 hr were cultured in the absence of FBS (0% FBS) for an additional 24 hr. The cells were then simulated with epidermal growth factor (EGF; 10 ng/ml) or insulin-like growth factor 1 (IGF-1; 10 ng/ml) for another 1 hr before being harvested for western blotting. Lysates were loaded into two gels due to sample well limits but the membranes were probed with same antibodies for equal duration and the proteins were detected under same exposure time.

(B) Western blotting of total lysates or subcellular fractions from SKUT2 endometrial cancer cells transfected with *PIK3R1*^{WT}, *PIK3R1*^{E160*}, *PIK3R1*^{R348*}, or *KRAS*^{G12D}. α-Tubulin (cytosolic), pan-cadherin (membrane), and histone H3 (nuclear) served as markers for purity of fractions.

(C and D) Immunohistochemical staining for p-ERK (C) and p-JNK (D) in four endometrial carcinomas carrying *PIK3R1*^{R348*} and 12 endometrial carcinomas without *PIK3R1*^{R348*} (control). Nuclei were counterstained in hematoxylin. Scale bar represents 50 μm.

See also Figure S2 and Table S4.

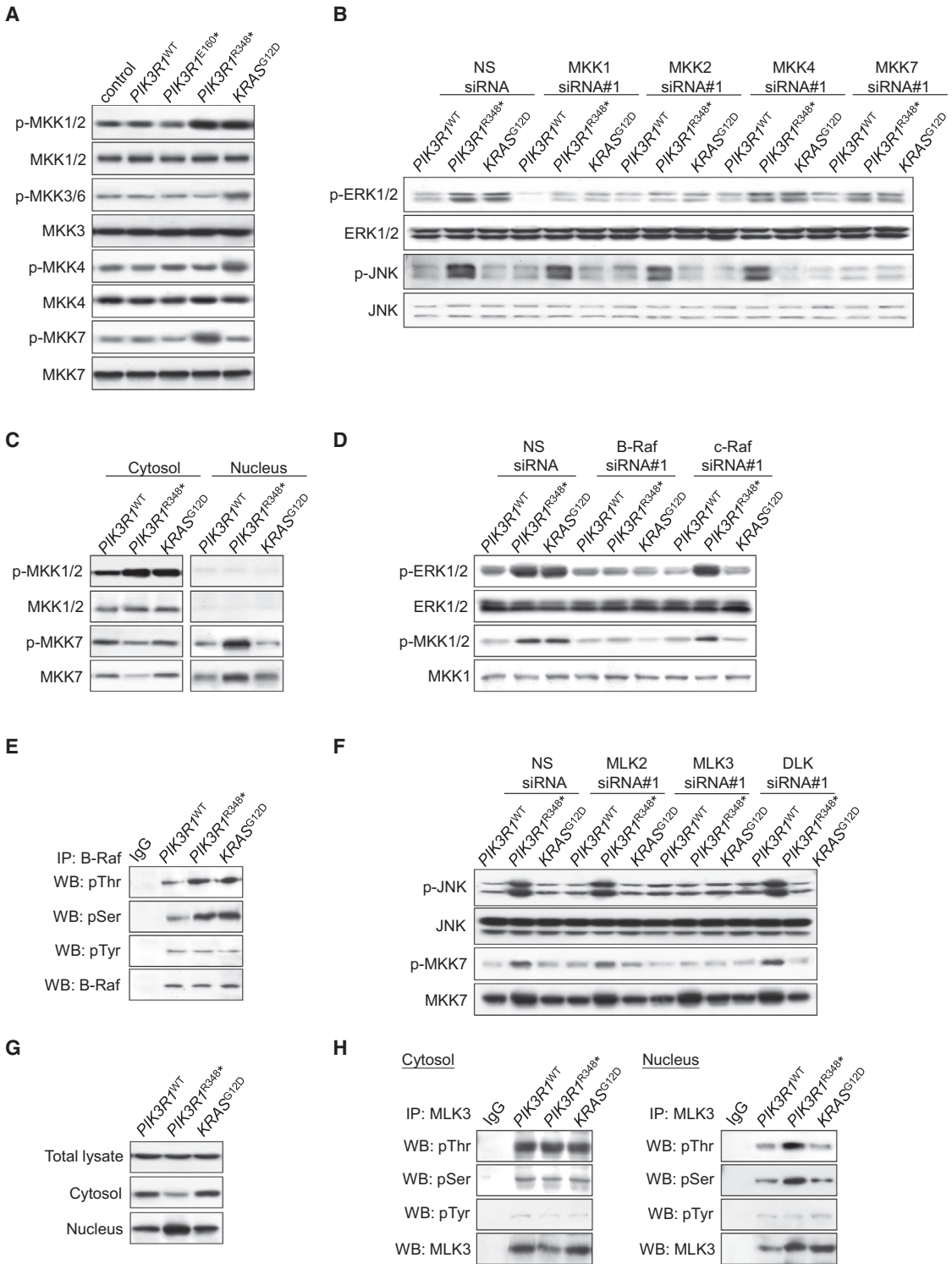

Figure 3. *PIK3R1*^{R348*} Selectively Activates B-Raf-MKK1/2-ERK and MLK3-MKK7-JNK Pathways

(A) Total lysates from transfected SKUT2 were analyzed with western blotting.

(B) Cells cotransfected with *PIK3R1*^{WT}, *PIK3R1*^{R348*} or *KRAS*^{G12D} and 20 nM siRNAs targeting the MKKs or nonspecific (NS) control for 72 hr were harvested for subcellcular fractionation. Western blots shown were from nuclear lysates.

(C) Transfected SKUT2 were harvested for subcellcular fractionation and western blotting.

(D) Cells were cotransfected with *PIK3R1*^{WT}, *PIK3R1*^{R348*}, or *KRAS*^{G12D} and 10 nM siRNAs targeting B-Raf, c-Raf, or NS control for 72 hr. Data shown are western blots of cytosolic lysates.

(legend continued on next page)

supported by p85α R348* and L370fs lacking the iSH2 domain that mediates association with p110. The N-terminal region of p85α is thought to contribute to PI3K activity-independent functions of *PIK3R1*. We and others have recently shown that p85α forms a homodimer that binds to and regulates PTEN (Cheung et al., 2011; Taniguchi et al., 2006). p85α also interacts with small GTPases of the Rho family to regulate cytokinesis (García et al., 2006). Moreover, *PIK3R1*^{WT} mediates insulin-induced activation of JNK via Cdc42 and MKK4 (Taniguchi et al., 2007). The signaling cascade by which *PIK3R1*^{R348*} activates JNK is MKK7-dependent and is distinct from that proposed for the actions of *PIK3R1*^{WT} (Taniguchi et al., 2007).

Perhaps the most striking neomorphic characteristic of p85α R348* and L370fs is the prominent nuclear localization that promotes JNK signaling. Nuclear translocation of the neomorphs requires an intact BH domain and is blocked by p85α SH2 domains. The p85α SH2 domains mediate interaction with cytoskeletal regulatory proteins such as FAK (Bachelot et al., 1996) and phosphotyrosine-containing peptides, such as receptor tyrosine kinases (Hellyer et al., 1998; McGlade et al., 1992; Pandey et al., 1994). Physical linkage to these cytoskeletal and membranous proteins may prohibit p85α from translocating into the nucleus. In a search for nuclear transport chaperones, we demonstrated that Rac1 and Cdc42, which bind p85α via its BH domain (Tolias et al., 1995; Zheng et al., 1994), were required for nuclear translocation of p85α R348*. Interestingly, both Rac1 and Cdc42, which carry canonical NLS (K-K/R-x-K/R), have been proposed to act as nuclear transport chaperones for STAT5 (Kawashima et al., 2006), SmgGDS (Lanning et al., 2003), p120 catenin (Lanning et al., 2003), and ACK (Ahmed et al., 2004). Rac1 also acts as transcriptional coactivator through associating with transcription factors in the nucleus (Buongiorno et al., 2008; Kawashima et al., 2006; Lanning et al., 2003) and nuclear Cdc42 regulates chromosome dynamics (Lagana et al., 2010; Yasuda et al., 2004). Nuclear import of Cdc42 and Rac1 may also be facilitated through binding to other effectors harboring NLS, such as PAR family members (Johansson et al., 2000). Indeed, as indicated in our gel filtration studies, Cdc42 and Rac1 are consistently present in large physical complexes.

Importantly, in addition to providing a physical link for nuclear localization of the complex, Cdc42 and Rac1 activity is required to induce ERK and JNK signaling cascades. Our data are consistent with Cdc42 and Rac1 increasing MLK3 activity, resulting in JNK activation (Teramoto et al., 1996). Although MLK3 has been shown to mediate B-Raf-induced ERK activation (Chadee and Kyriakis, 2004), it is unlikely in our model because *PIK3R1*^{R348*}-induced phosphorylation of MLK3 only occurred in the nucleus. Rather, *PIK3R1*^{R348*}-induced ERK activation most likely requires unidentified downstream effectors of Cdc42 or Rac1. In this regard, PAK, which is a Cdc42 and Rac1 target, has been demonstrated to activate the Raf/ERK cascade (Koh et al., 2009). The BH domain of p85α shares high homology to the Rho GTPase-activating protein domain of the breakpoint cluster region (bcr) protein, which inactivates Rho family proteins. There are conflicting data on the regulation of Cdc42 and Rac1 activity by p85α. Wild-type p85α has been shown to increase (Taniguchi et al., 2007), decrease (Chamberlain et al., 2004; Stankiewicz et al., 2010), or have no effect (Zheng et al., 1994) on the activity of Cdc42 or Rac1. It is possible that both an intact N terminus and functional SH2 domains are required for WT p85α to regulate the activity of Rho GTPases (Taniguchi et al., 2007). We also found that p85α R348*, which lacks SH2 domains, was not sufficient to alter GTP binding or expression level of Cdc42 or Rac1 in either the cytosol or nucleus (our unpublished observations). It is possible that basal activity of Cdc42 and Rac1 is sufficient to support the effects of *PIK3R1*^{R348*}.

p85α R348* and L370fs appear to be scaffolds that coordinate the formation of a stable MLK3/MKK7/JNK1/JNK2 complex. From structural features, we speculate that p85α R348* and L370fs directly bind MLK3 through conserved proline-rich and SH3 domains (Zhang and Gallo, 2001). Interestingly, the SH3 domain of p85α shares high homology with that of JIP1, which is a known scaffold for the MLK/MKK/JNK complex and binds MKK7 via its SH3 domain (Dickens et al., 1997). Thus the SH3 domain in p85α R348* and L370fs may also bind MKK7. Because p85α lacks an obvious consensus JNK-binding domain, JNK is likely to be tethered to the complex through an interaction with MKK7 or other intermediary proteins. Moreover, as JIP-1 causes cytosolic retention of JNK (Dickens et al., 1997), it is conceivable that p85α R348* and L370fs displace the cytosolic MLK3/MKK7/JNK from the JIP1 scaffold, allowing nuclear translocation. The recruitment and stabilization of a MLK3/MKK7/JNK1/JNK2 complex in the nucleus may be required for nuclear JNK activation. Indeed, while the p85α R348*/Rac1/Cdc42/MLK3/MKK7/JNK1/JNK2 complex can be detected in the cytosol, particularly when R348* is excluded from the nucleus, phosphorylated forms of JNK, MLK3, and MKK7 are highly enriched in the nuclear compartment. Thus, either an active complex is formed in the cytosol and then rapidly translocated to the nucleus or MKK7 and JNK1/2 are rapidly dephosphorylated in the cytosol. Alternatively, phosphorylation of complex components occurs primarily in the nucleus. Differential binding partners in the complex between cytosol and nucleus may account for this specificity. Indeed, although we demonstrated the presence of multiple molecules in the complex in the cytosol and the nucleus, the sizes of the complexes were different in both compartments. Furthermore, the large size of the complexes suggests that additional molecules are likely present in the complex. Their identities as well as their roles in the functional activity of the neomorphs remain to be identified.

(E) Total lysates from transfected SKUT2 were harvested for immunoprecipitation (IP) with anti-B-Raf antibody and western blotting (WB). IP with anti-IgG was used as control.
(F) Cells cotransfected with *PIK3R1*^{WT}, *PIK3R1*^{R348*}, or *KRAS*^{G12D} and 20 nM siRNAs targeting MLK2, MLK3, DLK (40 nM), or NS control for 72 hr were harvested for subcellular fractionation. Western blots shown were from nuclear lysates.
(G) Western blots for MLK3 in total lysates, cytosolic and nuclear fractions from transfected SKUT2.
(H) Western blots of IP with anti-MLK3 antibody using cytosolic and nuclear extracts from transfected SKUT2.
See also Figure S3.

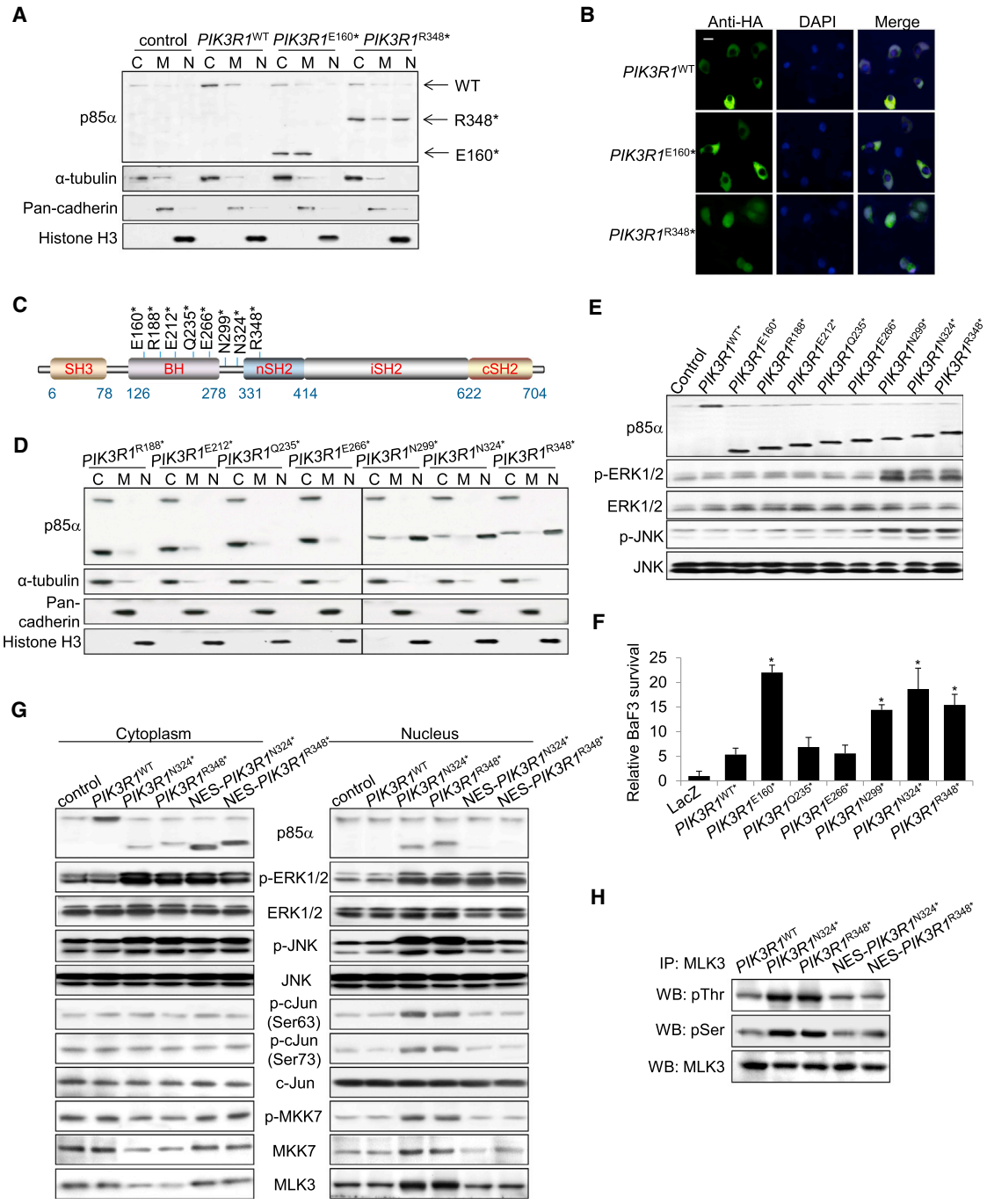

Figure 4. p85α R348* Localizes to the Nucleus and Activates MLK3-MKK7-JNK Signaling in the Nucleus

(A and B) SKUT2 cells transfected with HA-tagged *PIK3R1*^{WT}, *PIK3R1*^{E160*}, or *PIK3R1*^{R348*} were harvested for subcellular fractionation and western blotting (C, cytosolic; M, membrane; N, nuclear) (A) or immunostaining using anti-HA (green) antibody (B). DAPI was used for nuclear staining. "Merge" indicates combined images. Scale bar represents 10 μm.

(C) Schematic illustration of *PIK3R1* truncation mutations upstream of R348*.

(D and E) Cell lysates from SKUT2 cells transfected with indicated mutants were subjected for subcellular fractionation as in (A) (D) or western blotting (E).

(F) BaF3 cells transfected with *PIK3R1*^{WT} or *PIK3R1* mutant were cultured without IL-3 for 4 weeks prior to viability assay. Means (±SD) of triplicates from three independent experiments are shown.

(G and H) SKUT2 transfected with *PIK3R1*^{WT}, *PIK3R1*^{N324*}, *PIK3R1*^{R348*}, or *PIK3R1*^{N324*} and *PIK3R1*^{R348*} fused with nucleus export signal (NES) were harvested for subcellular fractionation and WB (G) or IP with anti-MLK3 antibody in nuclear extract and analyzed by WB (H). *$p < 0.05$, compared with *PIK3R1*^{WT}. Control, parental SKUT2.

See also Figure S4.

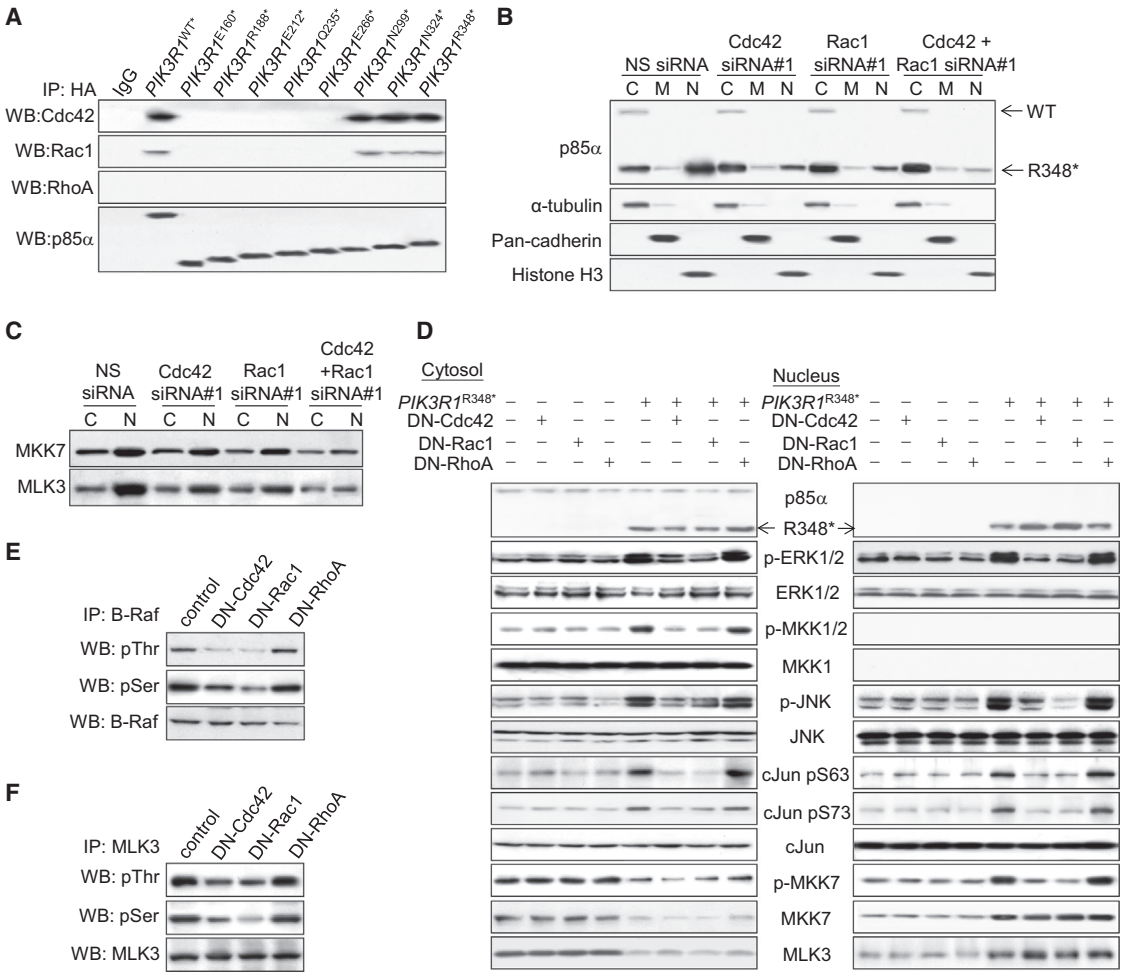

Figure 5. Cdc42 and Rac1 Mediate Nuclear Entry of p85α R348* and Activation of ERK and JNK Signaling Cascades by p85α R348*

(A) Total lysates from SKUT2 transfected with HA-tagged *PIK3R1*^{WT} or mutants were harvested for IP with anti-HA antibody and WB. IP with anti-IgG was used as control.

(B and C) Cells cotransfected with *PIK3R1*^{R348*} and 20 nM each of the indicated siRNAs for 72 hr were harvested for subcellular fractionation (C, cytosolic; M, membrane; N, nuclear) and WB.

(D–F) Cells cotransfected with *PIK3R1*^{R348*} and dominant negative (DN)-Cdc42, -Rac1, or -RhoA for 72 hr were harvested for subcellular fractionation (D) or total lysates used for IP with anti-B-Raf antibody (E) or nuclear lysates used for IP with anti-MLK3 antibody (F).

See also Figure S5.

Signaling specificity, such as strength, duration, and location of activation, determines the functional consequences of MAPK signaling (Inder et al., 2008). The pro- and anti-apoptotic signals transmitted by JNK are an archetype of this phenomenon (Dhanasekaran and Reddy, 2008). We found that activation of JNK in the nucleus renders cells resistant to FAS-induced apoptosis. Thus, exclusive activation of JNK in the nucleus may serve to explain the functional consequences of the nuclear localization of p85α R348* and L370fs and the selection of these mutations during tumorigenesis. Blocking ERK and JNK inhibited *PIK3R1*^{R348*}- and *PIK3R1*^{L370fs}-induced tumorigenic phenotypes. Indeed, whether combined inhibition of the PI3K pathway, MEK, and/or JNK signaling are required to achieve maximal suppression of the tumorigenic function of these *PIK3R1* neomorphs warrants further study and will provide preclinical data required to develop trials to treat patients with aberrations in this region of *PIK3R1*. In endometrial cancer, comutations in PI3K pathway members occur at frequencies significantly higher than predicted, suggesting that comutations in different components of the PI3K pathway may cooperate for efficient transformation (Cheung et al., 2011; Oda et al., 2008). Interestingly, *PTEN* or *PIK3CA* mutations co-occur at a frequency higher than expected with *PIK3R1*^{R348*} in both our in-house (five of five *PIK3R1*^{R348*}-tumors) and TCGA endometrial cancer cohorts (seven of eight *PIK3R1*^{R348*}-tumors). In contrast, *KRAS* mutation and *PIK3R1*^{R348*} did not co-occur in our in-house cohort (zero of five *PIK3R1*^{R348*}-tumors) and they co-occurred at the expected frequency based on the prevalence of each independent mutation in TCGA cohort (four of eight *PIK3R1*^{R348*}-tumors).

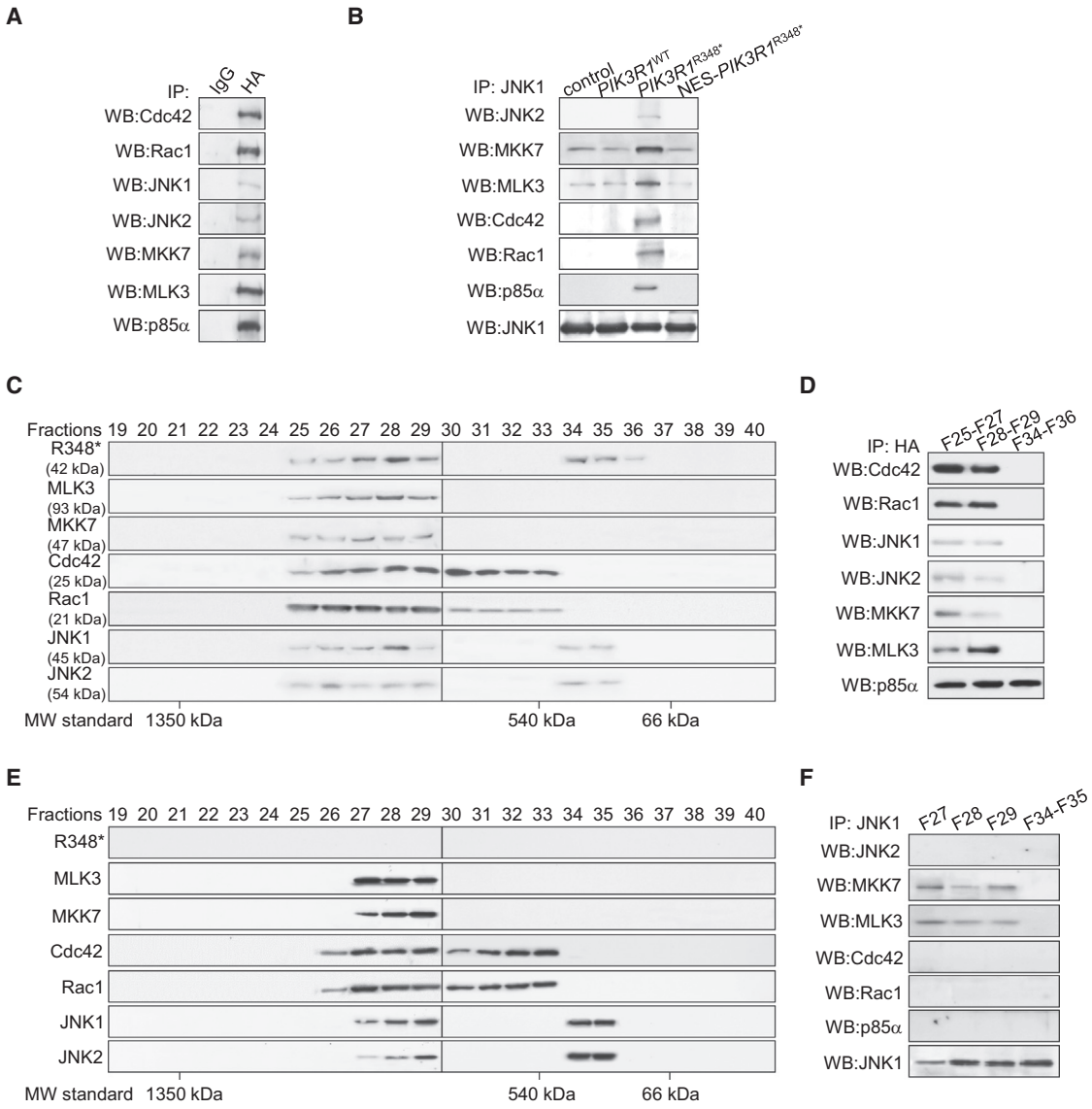

Figure 6. p85α R348* Acts as a Scaffold to Assemble a Cdc42/Rac1/MLK3/MKK7/JNK1/JNK2 Complex

(A) Nuclear lysates from SKUT2 cells transfected with HA-tagged *PIK3R1*^{R348*} were subjected to IP with anti-HA antibody and WB.

(B) Nuclear lysates from SKUT2 transfected with HA-tagged *PIK3R1*^{WT}, *PIK3R1*^{R348*}, or nucleus export signal (NES)-fused *PIK3R1*^{R348*} were subjected to IP with anti-JNK1 antibody.

(C and D) Nuclear extract from SKUT2 transfected with HA-tagged *PIK3R1*^{R348*} was fractionated using gel filtration column. The indicated fractions were analyzed with WB (C) or pooled for IP with anti-HA antibody (D).

(E and F) Nuclear extract from SKUT2 transfected with HA-tagged NES-*PIK3R1*^{R348*} was fractionated using gel filtration. The indicated fractions were analyzed (E) with WB or pooled for IP with anti-JNK1 antibody (F). F, fraction; MW, molecular weight.

See also Figure S6.

With the advent of therapies targeting the PI3K and MAPK pathways and genomic profiling, there is a tremendous interest in identifying biomarkers that can select cancer patients most likely to benefit from targeted therapy. The ability of *PIK3R1*^{R348*} and *PIK3R1*^{L370fs} to selectively activate the MEK and JNK pathways and to potentially bypass effects of PI3K pathway inhibitors similar to KRAS suggests that caution should be used in enrolling these patients into PI3K targeted clinical trials. It may be necessary to treat patients with *PIK3R1*^{R348*}, *PIK3R1*^{L370fs}, or neighboring *PIK3R1* mutations using similar approaches to patients with combined RAS and PI3K pathway mutations, a common observation in endometrial and colon cancers. Finally, if neomorphic mutation is a generalizable phenomenon with many other mutations in cancer genes also acting as neomorphs, this provides a note of caution in the application of targeted therapies. In this case, it will be likely that the implementation of approaches to functionally characterize the effects of patient-specific mutations will be needed to fulfill the promise of

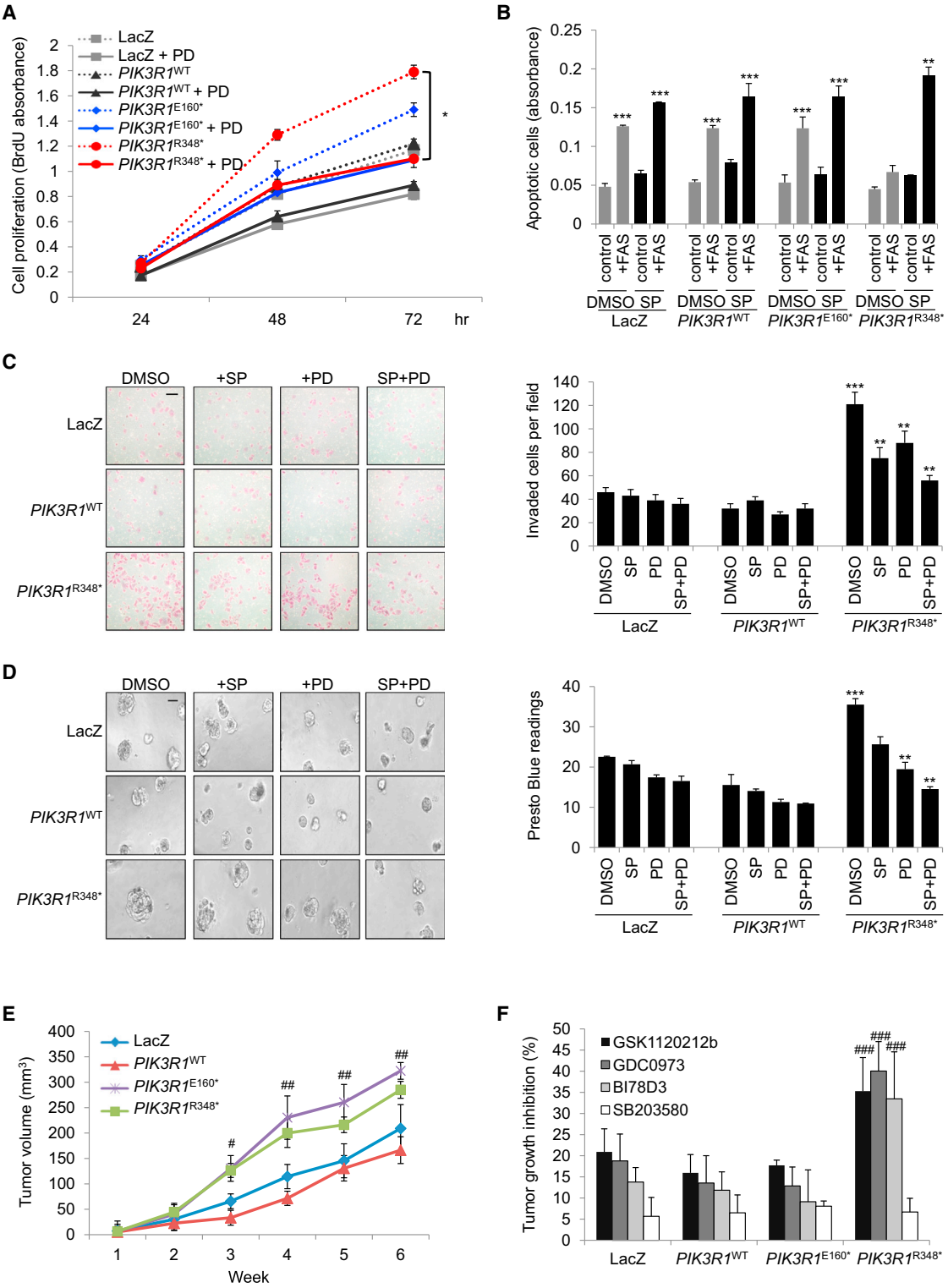

Figure 7. *PIK3R1*^{R348*} Promotes Malignant Phenotypes In Vitro and In Vivo through ERK and JNK

(A) SKUT2 stably expressing LacZ, *PIK3R1*^{WT}, *PIK3R1*^{E160*}, or *PIK3R1*^{R348*} were cultured in medium containing 1% FBS with or without MEK inhibitor PD0325901 (PD) at 20 nM. DMSO served as negative control. Cell proliferation was determined at 24, 48, and 72 hr after seeding.

(B) Stable SKUT2 were cultured in medium containing 5% FBS (control) or anti-Fas antibody (+FAS) with or without JNK inhibitor SP600125 (SP) at 20 μM for 72 hr before apoptosis assay.

(legend continued on next page)

personalized cancer therapy and importantly to prevent untoward consequences of targeted therapy.

EXPERIMENTAL PROCEDURES

Cell Culture and Reagents

Endometrial cancer cell lines and BaF3 were cultured as reported (Cheung et al., 2011). Ovarian cancer cell line OVK18 from the Riken BioResource Center (Japan) was cultured in minimum essential media with 10% fetal bovine serum (FBS). Generation of stable isogenic SKUT2 cell lines is described in the Supplemental Experimental Procedures. Stable BaF3 cell lines were selected with blasticidin (20 μg/ml) and IL-3 withdrawal and were maintained in medium without IL-3. IGF-1 and EGFR ligands were from R&D Systems. SP600125 and PD0325901 for in vitro assays were from Sigma-Aldrich. The 145-compound library was obtained from the John S. Dunn Gulf Coast Consortium for Chemical Genomics. For in vivo studies, GSK1120212B and GDC0973 were from the PI3K in Women's Cancer Stand up to Cancer Project; BI78D3 was from Santa Cruz Biotechnology. PD0325901 and SB203580 were from LC Laboratories.

BaF3 Cytotoxicity Assay

The day before treatment, stable BaF3 cells (1×10^4) were seeded in 96-well plates in medium with or without IL-3. Cells were treated with DMSO or inhibitors (1 nM to 10 μM) in the presence or absence of IL-3 for 72 hr. Cell viability was determined using PrestoBlue (Promega). Two independent experiments, each in duplicate, were performed.

Cell Extract Preparation, Immunoprecipitation, and Western Blotting

Cytosol, membrane, and nuclear fractions were prepared using FractionPREP Cell Fractionation kit (BioVision). Whole-cell lysates for western blotting were extracted with RIPA (25 mM Tris-HCl pH 7.6, 150 mM NaCl, 1% NP-40, 1% sodium deoxycholate, 0.1% SDS, protease, and phosphatase inhibitor cocktail). Cell lysates (25 μg) were loaded onto SDS-PAGE and transferred to a polyvinylidene fluoride membrane and protein expression was depicted with an enhanced chemiluminescence western blot detection kit (Amersham Biosciences). Whole-cell lysates for immunoprecipitation were prepared using lysis buffer containing 0.5% NP-40, 50 mM Tris pH 7.4, 150 mM NaCl, 5 mM EDTA pH 8, and protease inhibitors. Nuclear extracts for immunoprecipitation was prepared using Nuclear Complex Co-IP Kit (Active motif). The lysates were precleared by incubating with 1:1 slurry of protein A/G agarose (Santa Cruz Biotechnology) for 1 hr at 4°C, and then immunoprecipitated with antibodies against HA, B-Raf, MLK3, or JNK1 overnight at 4°C. The immune complexes were collected by incubation with protein A/G agarose for 4 hr before being resolved by SDS-PAGE. Normal IgG was used as negative control. Antibodies used are listed in the Supplemental Experimental Procedures.

Human Endometrial Tumor Samples and Immunohistochemistry

The endometrial cancer patient samples have been described previously (Cheung et al., 2011). After informed consent, patient materials were collected according to an Institutional Review Board-approved protocol at MD Anderson Cancer Center (MDACC). Immunohistochemistry was performed in the Histology and Tissue Processing Facility Core at MDACC. Intensity of nuclear staining was evaluated by a pathologist (Dr. R. Broaddus). All histological studies were performed in a blinded manner with regard to the sample genetic context.

Mice

All animal experiments were approved by MDACC's Institutional Animal Care and Use Committee. Animal care was followed according to institutional guidelines. Detailed experimental procedures are provided in the Supplemental Experimental Procedures.

Statistical Analysis

All experiments were independently repeated at least twice. Data of the in vitro assays were derived from triplicates of three independent experiments and are presented as means ± SD. The significance of differences was analyzed with Student's t test. Significance was accepted at the 0.05 level of probability ($p < 0.05$).

Additional experimental protocols are described in the Supplemental Experimental Procedures.

SUPPLEMENTAL INFORMATION

Supplemental Information includes Supplemental Experimental Procedures, seven figures, and four tables and can be found with this article online at http://dx.doi.org/10.1016/j.ccell.2014.08.017.

ACKNOWLEDGMENTS

We thank Dr. Jinsong Liu for the *KRAS*^{G12D} plasmids. This work was supported by National Cancer Institute (NCI) 2P50 CA098258-06 to R.R.B. and G.B.M.; NCI U01 CA168394 to G.B.M.; Stand Up to Cancer/AACR Dream Team Translational Cancer Research Grant SU2C-AACR-DT0209 to G.B.M.; MD Anderson Cancer Center Uterine SPORE Career Development Award and the Lorraine Dell Program in Bioinformatics for Personalization of Cancer Medicine to H.L.; TCGA GDAC grant (NIH/NCI U24 CA143883) to G.B.M. and H.L.; training grant from the Keck Center Computational Cancer Biology Training Program of the Gulf Coast Consortia (CPRIT grant no. RP101489) to L.W.T.; NIH High-End Instrumentation program grant (1S10OD012304-01) and CPRIT Core Facility Grant (RP130397) for supporting the Proteomics and Metabolomics Facility in MD Anderson Cancer Center; and the CCSG RPPA core, the Characterized Cell Line Core, and the DNA analysis facility (funded by NCI no. CA16672) in the MD Anderson Cancer Center. G.B.M. is a paid consultant for Astra Zeneca; he has received sponsored research support from Astra Zeneca and GSK.

Received: June 21, 2013
Revised: June 5, 2014
Accepted: August 26, 2014
Published: October 2, 2014

REFERENCES

Ahmed, I., Calle, Y., Sayed, M.A., Kamal, J.M., Rengaswamy, P., Manser, E., Meiners, S., and Nur-E-Kamal, A. (2004). Cdc42-dependent nuclear translocation of non-receptor tyrosine kinase, ACK. Biochem. Biophys. Res. Commun. *314*, 571–579.

(C) Representative images (left) and mean number of invaded cells of five fields at magnification of 40× (right) of indicated SKUT2 cells in the presence of indicated inhibitors.
(D) Representative images (left) and cell viability (right) of indicated SKUT2 cells grown in 3D culture for 6 days before being treated with SP or PD or combination for another 3 days.
(E) Cells were subcutaneously injected into mouse flank regions (n = 12/group). Tumor volume was measured weekly.
(F) Tumor-bearing mice were treated with vehicles, MEK inhibitor GSK1120212b or GDC0973, JNK inhibitor BI78D3, or p38 MAPK inhibitor SB203580. Tumor growth inhibition percentages were calculated and presented in the graph.
Scale bars represent 50 μm (C and D). All in vitro assays were performed with two independent stable clones yielding similar results. Data (means ± SD) of clone 1 of triplicates from three independent experiments are shown. All in vivo data are represented as mean ± SEM. *$p < 0.05$; **$p < 0.05$ compared with *PIK3R1*^{R348*} DMSO control; ***$p < 0.05$ compared with *PIK3R1*^{WT} DMSO control. $^{\#}p < 0.05$ compared with *PIK3R1*^{WT} at same time point; $^{\#\#}p < 0.01$ compared with *PIK3R1*^{WT} at same time point; $^{\#\#\#}p < 0.05$ compared with *PIK3R1*^{WT} treated with corresponding inhibitor. See also Figure S7.

Bachelot, C., Rameh, L., Parsons, T., and Cantley, L.C. (1996). Association of phosphatidylinositol 3-kinase, via the SH2 domains of p85, with focal adhesion kinase in polyoma middle t-transformed fibroblasts. Biochim. Biophys. Acta *1311*, 45–52.

Buongiorno, P., Pethe, V.V., Charames, G.S., Esufali, S., and Bapat, B. (2008). Rac1 GTPase and the Rac1 exchange factor Tiam1 associate with Wnt-responsive promoters to enhance beta-catenin/TCF-dependent transcription in colorectal cancer cells. Mol. Cancer *7*, 73.

Cerami, E., Gao, J., Dogrusoz, U., Gross, B.E., Sumer, S.O., Aksoy, B.A., Jacobsen, A., Byrne, C.J., Heuer, M.L., Larsson, E., et al. (2012). The cBio cancer genomics portal: an open platform for exploring multidimensional cancer genomics data. Cancer Discov *2*, 401–404.

Chadee, D.N., and Kyriakis, J.M. (2004). MLK3 is required for mitogen activation of B-Raf, ERK and cell proliferation. Nat. Cell Biol. *6*, 770–776.

Chamberlain, M.D., Berry, T.R., Pastor, M.C., and Anderson, D.H. (2004). The p85alpha subunit of phosphatidylinositol 3′-kinase binds to and stimulates the GTPase activity of Rab proteins. J. Biol. Chem. *279*, 48607–48614.

Chen, L.L., Trent, J.C., Wu, E.F., Fuller, G.N., Ramdas, L., Zhang, W., Raymond, A.K., Prieto, V.G., Oyedeji, C.O., Hunt, K.K., et al. (2004). A missense mutation in KIT kinase domain 1 correlates with imatinib resistance in gastrointestinal stromal tumors. Cancer Res. *64*, 5913–5919.

Cheung, L.W., Hennessy, B.T., Li, J., Yu, S., Myers, A.P., Djordjevic, B., Lu, Y., Stemke-Hale, K., Dyer, M.D., Zhang, F., et al. (2011). High frequency of PIK3R1 and PIK3R2 mutations in endometrial cancer elucidates a novel mechanism for regulation of PTEN protein stability. Cancer Discov *1*, 170–185.

Cuevas, B.D., Lu, Y., Mao, M., Zhang, J., LaPushin, R., Siminovitch, K., and Mills, G.B. (2001). Tyrosine phosphorylation of p85 relieves its inhibitory activity on phosphatidylinositol 3-kinase. J. Biol. Chem. *276*, 27455–27461.

Dérijard, B., Raingeaud, J., Barrett, T., Wu, I.H., Han, J., Ulevitch, R.J., and Davis, R.J. (1995). Independent human MAP-kinase signal transduction pathways defined by MEK and MKK isoforms. Science *267*, 682–685.

Dhanasekaran, D.N., and Reddy, E.P. (2008). JNK signaling in apoptosis. Oncogene *27*, 6245–6251.

Dickens, M., Rogers, J.S., Cavanagh, J., Raitano, A., Xia, Z., Halpern, J.R., Greenberg, M.E., Sawyers, C.L., and Davis, R.J. (1997). A cytoplasmic inhibitor of the JNK signal transduction pathway. Science *277*, 693–696.

Etienne-Manneville, S., and Hall, A. (2002). Rho GTPases in cell biology. Nature *420*, 629–635.

Gallo, K.A., and Johnson, G.L. (2002). Mixed-lineage kinase control of JNK and p38 MAPK pathways. Nat. Rev. Mol. Cell Biol. *3*, 663–672.

García, Z., Silio, V., Marqués, M., Cortés, I., Kumar, A., Hernandez, C., Checa, A.I., Serrano, A., and Carrera, A.C. (2006). A PI3K activity-independent function of p85 regulatory subunit in control of mammalian cytokinesis. EMBO J. *25*, 4740–4751.

Hellyer, N.J., Cheng, K., and Koland, J.G. (1998). ErbB3 (HER3) interaction with the p85 regulatory subunit of phosphoinositide 3-kinase. Biochem. J. *333*, 757–763.

Inder, K., Harding, A., Plowman, S.J., Philips, M.R., Parton, R.G., and Hancock, J.F. (2008). Activation of the MAPK module from different spatial locations generates distinct system outputs. Mol. Biol. Cell *19*, 4776–4784.

Johansson, A., Driessens, M., and Aspenström, P. (2000). The mammalian homologue of the Caenorhabditis elegans polarity protein PAR-6 is a binding partner for the Rho GTPases Cdc42 and Rac1. J. Cell Sci. *113*, 3267–3275.

Kandoth, C., Schultz, N., Cherniack, A.D., Akbani, R., Liu, Y., Shen, H., Robertson, A.G., Pashtan, I., Shen, R., Benz, C.C., et al.; Cancer Genome Atlas Research Network (2013). Integrated genomic characterization of endometrial carcinoma. Nature *497*, 67–73.

Kawashima, T., Bao, Y.C., Nomura, Y., Moon, Y., Tonozuka, Y., Minoshima, Y., Hatori, T., Tsuchiya, A., Kiyono, M., Nosaka, T., et al. (2006). Rac1 and a GTPase-activating protein, MgcRacGAP, are required for nuclear translocation of STAT transcription factors. J. Cell Biol. *175*, 937–946.

Koh, W., Sachidanandam, K., Stratman, A.N., Sacharidou, A., Mayo, A.M., Murphy, E.A., Cheresh, D.A., and Davis, G.E. (2009). Formation of endothelial lumens requires a coordinated PKCepsilon-, Src-, Pak- and Raf-kinase-dependent signaling cascade downstream of Cdc42 activation. J. Cell Sci. *122*, 1812–1822.

Lagana, A., Dorn, J.F., De Rop, V., Ladouceur, A.M., Maddox, A.S., and Maddox, P.S. (2010). A small GTPase molecular switch regulates epigenetic centromere maintenance by stabilizing newly incorporated CENP-A. Nat. Cell Biol. *12*, 1186–1193.

Lanning, C.C., Ruiz-Velasco, R., and Williams, C.L. (2003). Novel mechanism of the co-regulation of nuclear transport of SmgGDS and Rac1. J. Biol. Chem. *278*, 12495–12506.

Lutzky, J., Bauer, J., and Bastian, B.C. (2008). Dose-dependent, complete response to imatinib of a metastatic mucosal melanoma with a K642E KIT mutation. Pigment Cell Melanoma Res *21*, 492–493.

Lynch, T.J., Bell, D.W., Sordella, R., Gurubhagavatula, S., Okimoto, R.A., Brannigan, B.W., Harris, P.L., Haserlat, S.M., Supko, J.G., Haluska, F.G., et al. (2004). Activating mutations in the epidermal growth factor receptor underlying responsiveness of non-small-cell lung cancer to gefitinib. N. Engl. J. Med. *350*, 2129–2139.

McGlade, C.J., Ellis, C., Reedijk, M., Anderson, D., Mbamalu, G., Reith, A.D., Panayotou, G., End, P., Bernstein, A., Kazlauskas, A., et al. (1992). SH2 domains of the p85 alpha subunit of phosphatidylinositol 3-kinase regulate binding to growth factor receptors. Mol. Cell. Biol. *12*, 991–997.

Murga, C., Zohar, M., Teramoto, H., and Gutkind, J.S. (2002). Rac1 and RhoG promote cell survival by the activation of PI3K and Akt, independently of their ability to stimulate JNK and NF-kappaB. Oncogene *21*, 207–216.

Ness, R.B. (2003). Endometriosis and ovarian cancer: thoughts on shared pathophysiology. Am. J. Obstet. Gynecol. *189*, 280–294.

Oda, K., Okada, J., Timmerman, L., Rodriguez-Viciana, P., Stokoe, D., Shoji, K., Taketani, Y., Kuramoto, H., Knight, Z.A., Shokat, K.M., and McCormick, F. (2008). PIK3CA cooperates with other phosphatidylinositol 3′-kinase pathway mutations to effect oncogenic transformation. Cancer Res. *68*, 8127–8136.

Pandey, A., Lazar, D.F., Saltiel, A.R., and Dixit, V.M. (1994). Activation of the Eck receptor protein tyrosine kinase stimulates phosphatidylinositol 3-kinase activity. J. Biol. Chem. *269*, 30154–30157.

Quayle, S.N., Lee, J.Y., Cheung, L.W., Ding, L., Wiedemeyer, R., Dewan, R.W., Huang-Hobbs, E., Zhuang, L., Wilson, R.K., Ligon, K.L., et al. (2012). Somatic mutations of PIK3R1 promote gliomagenesis. PLoS ONE *7*, e49466.

Rodriguez-Viciana, P., Warne, P.H., Dhand, R., Vanhaesebroeck, B., Gout, I., Fry, M.J., Waterfield, M.D., and Downward, J. (1994). Phosphatidylinositol-3-OH kinase as a direct target of Ras. Nature *370*, 527–532.

Stankiewicz, T.E., Haaning, K.L., Owens, J.M., Jordan, A.S., Gammon, K., Bruns, H.A., and McDowell, S.A. (2010). GTPase activating protein function of p85 facilitates uptake and recycling of the beta1 integrin. Biochem. Biophys. Res. Commun. *391*, 443–448.

Taniguchi, C.M., Tran, T.T., Kondo, T., Luo, J., Ueki, K., Cantley, L.C., and Kahn, C.R. (2006). Phosphoinositide 3-kinase regulatory subunit p85alpha suppresses insulin action via positive regulation of PTEN. Proc. Natl. Acad. Sci. USA *103*, 12093–12097.

Taniguchi, C.M., Aleman, J.O., Ueki, K., Luo, J., Asano, T., Kaneto, H., Stephanopoulos, G., Cantley, L.C., and Kahn, C.R. (2007). The p85alpha regulatory subunit of phosphoinositide 3-kinase potentiates c-Jun N-terminal kinase-mediated insulin resistance. Mol. Cell. Biol. *27*, 2830–2840.

Teramoto, H., Coso, O.A., Miyata, H., Igishi, T., Miki, T., and Gutkind, J.S. (1996). Signaling from the small GTP-binding proteins Rac1 and Cdc42 to the c-Jun N-terminal kinase/stress-activated protein kinase pathway. A role for mixed lineage kinase 3/protein-tyrosine kinase 1, a novel member of the mixed lineage kinase family. J. Biol. Chem. *271*, 27225–27228.

Tolias, K.F., Cantley, L.C., and Carpenter, C.L. (1995). Rho family GTPases bind to phosphoinositide kinases. J. Biol. Chem. *270*, 17656–17659.

Tournier, C., Whitmarsh, A.J., Cavanagh, J., Barrett, T., and Davis, R.J. (1997). Mitogen-activated protein kinase kinase 7 is an activator of the c-Jun NH2-terminal kinase. Proc. Natl. Acad. Sci. USA *94*, 7337–7342.

Ward, P.S., Patel, J., Wise, D.R., Abdel-Wahab, O., Bennett, B.D., Coller, H.A., Cross, J.R., Fantin, V.R., Hedvat, C.V., Perl, A.E., et al. (2010). The common

feature of leukemia-associated IDH1 and IDH2 mutations is a neomorphic enzyme activity converting alpha-ketoglutarate to 2-hydroxyglutarate. Cancer Cell *17*, 225–234.

Yasuda, S., Oceguera-Yanez, F., Kato, T., Okamoto, M., Yonemura, S., Terada, Y., Ishizaki, T., and Narumiya, S. (2004). Cdc42 and mDia3 regulate microtubule attachment to kinetochores. Nature *428*, 767–771.

Yu, J., Zhang, Y., McIlroy, J., Rordorf-Nikolic, T., Orr, G.A., and Backer, J.M. (1998). Regulation of the p85/p110 phosphatidylinositol 3′-kinase: stabilization and inhibition of the p110alpha catalytic subunit by the p85 regulatory subunit. Mol. Cell. Biol. *18*, 1379–1387.

Zhang, H., and Gallo, K.A. (2001). Autoinhibition of mixed lineage kinase 3 through its Src homology 3 domain. J. Biol. Chem. *276*, 45598–45603.

Zheng, Y., Bagrodia, S., and Cerione, R.A. (1994). Activation of phosphoinositide 3-kinase activity by Cdc42Hs binding to p85. J. Biol. Chem. *269*, 18727–18730.